# The Lyman-alpha emission-line profiles in high-redshift QSOs

*Mon. Not. R. astr. Soc.* (1982) **201**, 645–660

# The Lyman-alpha emission-line profiles in high-redshift QSOs

B. J. Wilkes and R. F. Carswell *Institute of Astronomy, Madingley Road, Cambridge CB3 0HA*

Received 1982 March 11; in original form 1981 September 23

**Summary.** High-resolution (~ 1 Å) spectra of six high-redshift QSOs were utilized in a study of the profile of the Ly$\alpha$ $\lambda$ 1215.67 Å emission line. The symmetry of the profile was studied after removing any absorption lines, which are mostly resolved at this resolution and after subtraction of N v $\lambda$1240 and Si II $\lambda$1263 emission from the observed blend. With one exception, Q2204 – 408, the Ly$\alpha$ profiles are symmetric to within the uncertainties of the procedure. It also became clear during the analysis that the profiles of the emission lines are not identical, in particular C IV $\lambda$1549 generally has weaker wings and peak than Ly$\alpha$ $\lambda$1216.

It is argued that either the motion of the broad-line region gas is not purely radial, or else most of the Ly$\alpha$ photons originate in optically-thin gas. Further implications of these results are discussed.

## 1 Introduction

The broad emission lines characteristic of the spectra of quasi-stellar objects (QSOs) and Seyfert galaxies are generally believed to arise in a region of photo-ionized gas surrounding a central source of non-thermal radiation (Strittmatter & Williams 1976). Model calculations (e.g. Baldwin & Netzer 1978; Davidson & Netzer 1979) for the broad-line region (BLR) imply gas which is optically thick to the Lyman continuum, with typical temperatures of $\sim 10^4$ K and densities of $10^{8.5}$–$10^{10.5}$ cm$^{-3}$, the upper limit being set by the strong presence of the semi-forbidden line [C III] $\lambda$1909, which would be de-excited at higher densities and the lower limit by the absence of broad [O III] $\lambda\lambda$4959, 5007 lines (MacAlpine 1976; Netzer 1976, 1977). Where it is observed the presence of He I $\lambda$5876 implies densities near the upper limit of this range (MacAlpine 1976). The intensities of high-excitation lines such as N v $\lambda$1240 and O VI $\lambda$1034 can be reproduced by invoking a second component of gas, probably optically thin and with a relatively high-ionization parameter (effectively the ratio of radiation flux density to electron density). (Davidson 1977; Netzer 1976.)

The covering factor of the gas is estimated to be small (~ 5 per cent) (Baldwin & Netzer 1978; Carswell & Ferland 1980; Smith *et al.* 1981) and although the detailed arrangement is as yet uncertain, it is likely that most of the gas is contained in a number of small clouds or

filaments (Davidson 1972; Shields, Oke & Sargent 1972). An observational lower limit to the number of components of gas, based on the lack of any clumpiness in the emission lines, is $\sim 10^4$ (Atwood, Baldwin & Carswell 1982) although theoretical estimates indicate a much higher number $> 10^{10}$.

The large widths of the emission lines (10 000 km $s^{-1}$) are assumed to be the consequence of bulk motion of the emitting gas; this may be random, orbital motion, pure expansion or contraction, or (most probably) some combination of all three.

In any geometric configuration involving optically-thick gas there is an indeterminate amount of neutral gas beyond the photo-ionized layer which is illuminated by the central radiation source. Absorption lines originating in this gas have not been unambiguously detected in the spectra of QSOs (Smith *et al.* 1981). The absence of this absorption and size arguments given by Carswell & Ferland (1980) suggest that the cross-section of the illuminated face of the gas clouds is small compared with the size of the continuum source. However, the presence of this neutral gas affects the radiative transfer of the photons with the result that the emissivity of each cloud is directionally dependent. (Ferland, Netzer & Shields 1979). The effect is particularly marked for Ly$\alpha$ photons, which suffer heavily from resonance scattering in the neutral gas, eventually escaping mainly through the ionized layer back towards the central source. Thus, the main contribution to the emission line comes from the gas on the far side of the QSO. It is immediately obvious that under these circumstances any bulk radial motion of the emitting gas will lead to strong asymmetry in the Ly$\alpha$ line, the sense of which is dependent upon the direction of flow. Since the effect on the other broad lines is small in comparison, it is possible to place limits on the amount of radial flow present in the BLR by studying the Ly$\alpha$ emission-line profile and comparing it with those of the other broad lines. Even if all the lines are asymmetric as a result of some bulk motions the Ly$\alpha$ profile should be markedly different.

In low-resolution data, the presence of both N v $\lambda$1240 blending into the red wing and the well-known forest of absorption lines eating into the violet wing is very likely to cause apparent asymmetry. In order to study the line unambiguously, high-resolution data ($\leqslant 2$ Å) is necessary, for the majority of the absorption lines are then resolved and their presence in the emission line can be allowed for. In this paper we report results obtained from studying the Ly$\alpha$/N v $\lambda$1240 feature (referred to here as the 1216 feature) in six QSOs using high-resolution spectral data. Possible implications of the results upon theories of the broad-line region (BLR) are discussed.

## 2 The observations

Spectra were obtained in 1979 November and 1980 April using the Image Photon Counting System (IPCS) (Boksenberg 1972, 1978) on the RGO spectrograph at the $f/8$ Cassegrain focus of the Anglo-Australian telescope. The spectrograph was used with a 150 groove $mm^{-1}$ grating blazed at 2.6 $\mu$m with a prism cross-disperser (40 grooves $mm^{-1}$ on a 2°.43 UBK7 prism) to separate the orders. Useful information was obtained for the object and sky spectra simultaneously in the fourth to seventh orders, using apertures separated by $\sim 20$ arcsec. The wavelength range and dispersions obtained are summarized in Table 1. A 225 $\mu$m (1.5 arcsec) slit was used, given a resolution of about three channels on the detector. Sky and object positions were interchanged at 1500 s intervals in order to correct for any asymmetries in the system response and comparison arc spectra for wavelength calibration recorded after each pair of such integrations.

The data were collected in a two-dimensional array of 2030 spectral channels by 90 spatial channels and subsequently extracted and analysed using the SERC STARLINK VAX

**Table 1.** Spectrograph properties.

| Order | Wavelength range | Dispersion (A ch$^{-1}$) |
|---|---|---|
| 4 | 5400–7060 | 1.0 |
| 5 | 4400–6000 | 0.8 |
| 6 | 3650–4900 | 0.67 |
| 7 | 3500–4200 | 0.57★ |

★ Response relatively poor.

computer at the Institute of Astronomy. The extraction programs used are similar to those used by Carswell *et al.* (1975), developed then for a similar spectrograph system. The data were corrected to a relative flux scale using standard star observations of white dwarfs for which Oke (1974) has published spectrophotometric data. The objects observed are listed in Table 2 with their mean redshift and total exposure time.

## 3 Analysis

In order to study the Ly$\alpha$ profile itself it was first necessary to remove the many absorption lines from the profile and also the N v λ1240 emission which is blended into the red wing of the feature. A fit for each 1216 blend was generated by first removing all the absorption lines by interpolating across them and then smoothing by 2–3 resolution elements to suppress the noise.

The N v λ1240 emission was removed from ther red wing using a de-blending technique and program developed by Baldwin & Netzer (1978). A synthetic fit to the 1216 feature was produced using another line in the spectrum known to be fairly free from absorption and blending itself, in all cases here the C IV λ1549 profile was used. While it is true that C IV λ1549 is itself a doublet, the separation is small compared with the linewidths in all the

**Table 2.** Objects observed.

| Object | RA | Dec | $z$ | Dwell time (s) | | Ref. |
|---|---|---|---|---|---|---|
| Q0000 – 398 | 00 00 30.3 | – 39 48 51 | 2.832 | 3 000 | | 1, 2 |
| Q0207 – 398 | 02 07 24.3 | – 39 53 50 | 2.815 | 3 000 | | 1, 2 |
| Q1101 – 264★ | 11 01 00.0 | – 26 29 08 | 2.143 | – | | 3, 4 |
| 1256 – 175 | 12 56 17.2 | – 17 34 31 | 2.061 | 6 000 | | – |
| 1331 + 170 | 13 31 10.0 | + 17 04 20 | 2.084 | 12 000 | | 5, 6, 7 |
| | | | | Lyα | C IV | |
| Q2204 – 408★ | 22 04 33.1 | – 40 51 39 | 3.170 | 12 000 | 16 000 | 3, 8 |

*Notes*

1. Osmer & Smith (1976).
2. Whelan, Smith & Carswell (1979).
3. Osmer & Smith (1977).
4. Carswell *et al.* (1982).
5. Baldwin & Netzer (1978).
6. Strittmatter *et al.* (1973).
7. Carswell et al. (1975).
8. Osmer (1979).

★ Although Q1104 – 264 and Q2204 – 408 were observed using the echelle, the data used here were obtained at higher resolution by Boksenberg, Carswell & Smith. These alternative data were used because the signal-to-noise ratio in the emission lines is much better.

QSOs analysed here, so it may be treated as a single line. This line was shifted to the wavelength of Ly$\alpha$ $\lambda$1215.67 and N v $\lambda\lambda$1238.81, 1242.8 (N v $\lambda$1240) and the relative strengths varied to find the optimum fit. It was then possible to subtract the part of the synthetic profile due to N v $\lambda$1240 from the observed 1216 blend, leaving the Ly$\alpha$ profile free from both absorption and blended emission lines.

Additionally, there is often an emission feature near 1265 Å which is usually attributed to a blend of Si II $\lambda\lambda$ 1260.4, 1265.0, (Si II $\lambda$1263). The identification of this feature is uncertain since theoretical calculations predict Si II to be weak. Another possibility is the UV-9 multiplet of Fe II, mean wavelength 1269.7 Å (Gaskell 1981). Where a 1265 Å feature was present in the data, a synthetic blend was produced using both alternatives; without exception the Si II identification yielded a better fit to the data.

The symmetry of these final profiles was studied by reflection about a variable line centre, facilitating easy comparison of the two halves of the profile. The redshift for the optimum position of the reflection point was compared with that for the other lines in the spectrum to check for possible shifts. The results are summarized in Table 3.

With the exception of Q0207 – 398 and Q2204 – 408 (see below) the C IV $\lambda$1549 profiles utilized for deblending were symmetric and relatively free from unambiguous absorption features. The signal-to-noise ratio is generally lower than in the 1216 blend so, for ease of comparison, smoothed fits to the profiles were made after allowing for absorption lines.

In general, where they are present, the low ionization lines O I $\lambda$1304 and C II $\lambda$1335 are redshifted with respect to the higher ionization lines (Table 3). This effect has also been reported by Gaskell (1981) and, for H$\alpha$, by Allen *et al.* (1982). Although comparisons are difficult due to the weakness of these lines it appears that, in this sample, their profiles are narrower than e.g. C IV $\lambda$1549 and C III] $\lambda$1909.

### *Notes on individual objects*

#### *Q0000 – 398 (Fig. 1)*

The C IV $\lambda$1549 profile is clearly different from that of Ly$\alpha$ (Fig. 1c), causing the hydrogen contribution to the red wing to be under-represented in the synthetic blend and thus the N v $\lambda$1240 component overestimated. The final Ly$\alpha$ profile is slightly enhanced in its blue wing (Fig. 1e) but this asymmetry is only marginally greater than the errors from the N v $\lambda$1240 subtraction (Fig. 1d). After studying the signal-to-noise ratio in the observed lines and including possible errors in the smoothed fits, we conclude that the profile is symmetric to within the margin of the errors. The slight excess at ~ 4850 Å is probably weak Si II $\lambda$1263 emission.

#### *Q0207 – 398 (Fig. 2)*

The C IV $\lambda$1549 profile has a marked blue skew (Fig. 2b). N v $\lambda$1240, which is fairly well-resolved from the Ly$\alpha$ line, also appears asymmetric in the same sense (Fig. 2a); as does O VI $\lambda$1034. Due to the bad mismatch of the C IV and Ly$\alpha$ profiles, the danger of errors in the production of the synthetic profile is increased, the red wing of the Ly$\alpha$ not being adequately represented (see Fig. 2c). The Ly$\alpha$ profile after subtraction of this blend is clearly symmetric to well within the error limits (Fig. 2d).

A rough comparison of N v $\lambda$1240 and C IV $\lambda$1549 is shown in Fig. 2(f); a synthetic blend using C IV $\lambda$1549 is shown (feint) superimposed upon the N v $\lambda$1240 and Si II $\lambda$1263 emission. The latter pair were isolated from the 1216 blend by subtracting a symmetric Ly$\alpha$ profile generated by reflecting the blue wing about the line centre. The discrepancy at

**Table 3.** Emission line parameters.

| Object | Lyα profile | $z$ (Lyα)[1] | $z$ (C IV λ1549)[2] | $\bar{z}$[3] | O I λ1304 | | C II λ1335 | | Intensity ratios | |
|---|---|---|---|---|---|---|---|---|---|---|
| | | | | | $z$ | $v$[4] (km s$^{-1}$) | $z$ | $v$ (km s$^{-1}$) | N V λ1240/Lyα | Si II λ1263/Lyα |
| Q0000 – 398 | Symmetric | 2.831 | 2.831 | 2.832 | 2.84 | 626 | – | – | 0.13 | 0.00 |
| Q0207 – 398 | Symmetric | 2.814 | 2.813 | 2.815 | 2.822 | 550 | 2.816 | 80 | 0.23 | 0.06 |
| Q1101 – 264 | Symmetric | 2.141 | 2.142 | 2.143 | – | – | – | – | 0.27 | 0.03 |
| 1256 – 175 | Symmetric | 2.060 | 2.059 | 2.061 | – | – | – | – | 0.09 | 0.07 |
| 1331 + 170 | Symmetric | 2.084 | 2.078 | 2.084 | – | – | – | – | 0.27 | 0.00 |
| Q2204 – 408 | Strong blue skew | 3.170 | 3.169 | 3.170 | 3.184 | 1007 | 3.178 | 576 | 0.35 | 0.12 |

*Notes.*
1. Redshift of Lyα is that of the reflection point used to test profile symmetry.
2. C IV λ1549 peak redshift.
3. Average redshift from all lines excluding Lyα and the low-ionization lines from O I, C II and Si II.
4. Velocity relative to high-ionization line redshift.

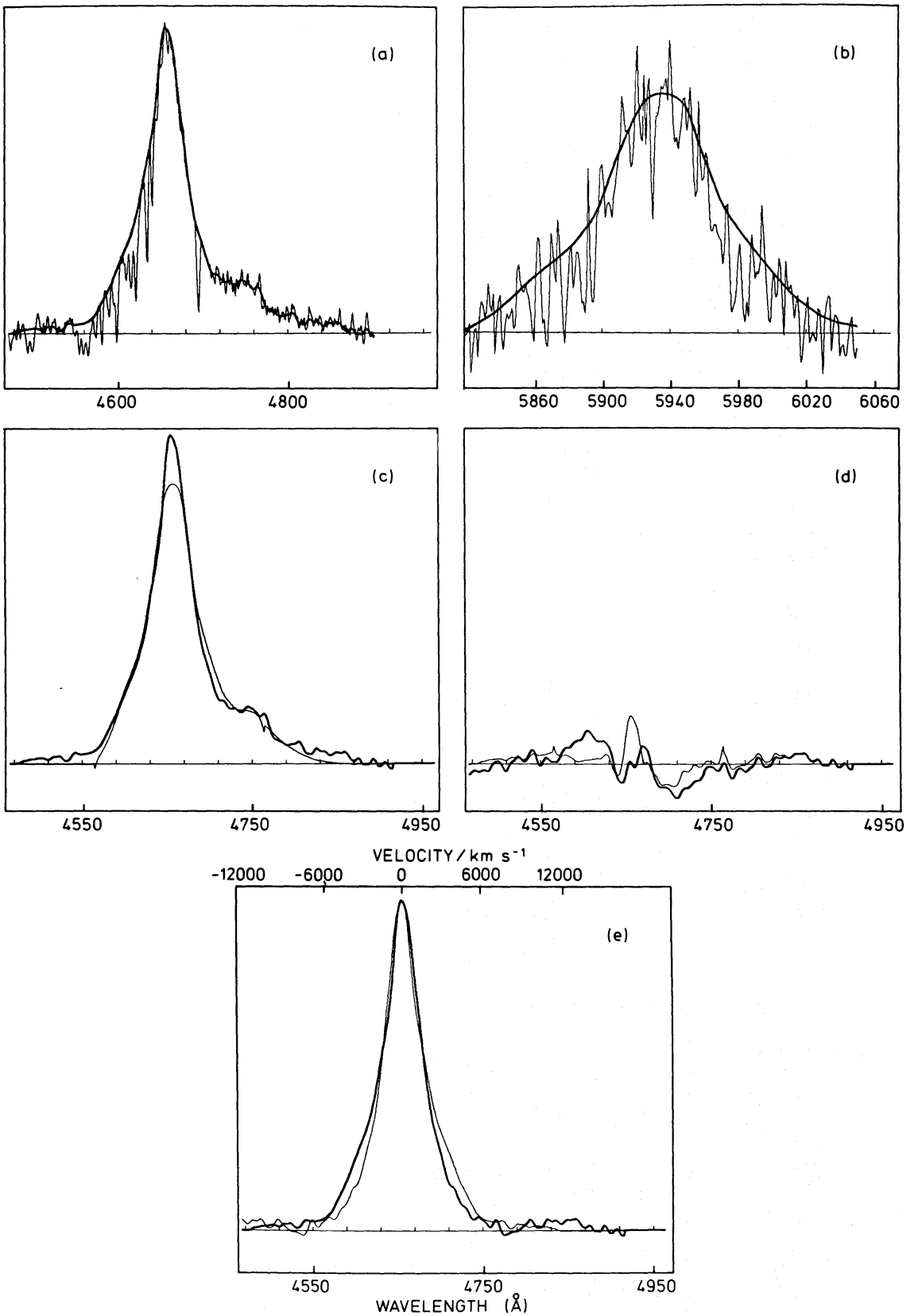


**Figure 1.** Line profile synthesis for Q0000–398. (a) A smoothed fit to the 1216 Å blend (reinforced line) superimposed on the original line profile. (b) A smoothed fit to the C IV λ1549 profile (reinforced line) and the original profile. (c) Synthetic 1216 blend (feint) obtained from the C IV λ1549 profile (see text) superimposed on the smooth fit to the blend. (d) Feint: the residual of real and synthetic 1216 blends (observed minus synthetic 1216 blends). Solid: the asymmetry of the final Ly$\alpha$ profile (Ly$\alpha$ profile minus its reflection about the line centre). The flux scale is as for (c) and (e). Comparison of these two residuals gives an indication of whether the apparent asymmetry is in excess of uncertainties introduced by the deblending procedure. (e) The final Ly$\alpha$ profile (reinforced) with its reflection superposed. Zero on the velocity scale indicates the adopted line centre.

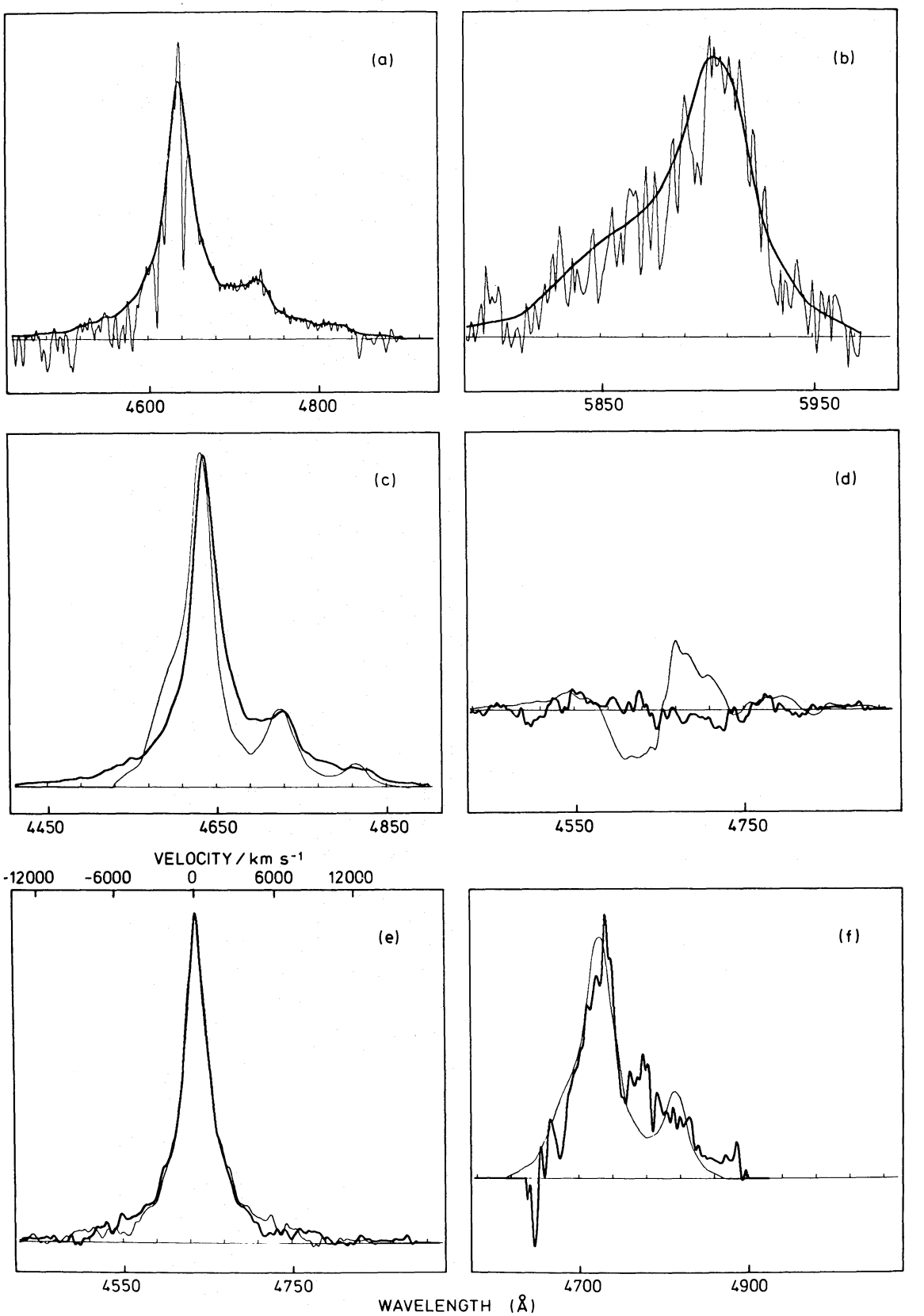


**Figure 2.** Line profile synthesis for Q0207 – 398. As Fig. 1. (a) Fit to 1216 blend, (b) fit to C IV λ1549, (c) synthetic (feint) and fitted 1216 blends, (d) synthetic blend residuals (feint) and asymmetry in Lyα, (e) final Lyα profile and its reflection (feint). Additionally, (f) the synthetic blend of N V λ1240 and Si II λ1263 (feint) superposed on the 1216 feature with the Lyα component subtracted out.

~ 4815 Å may be due to a real difference in the N v and C iv wings or a slight asymmetry in the Lyα wings.

*Q1101 – 264 (Fig. 3)*

It is clear from Fig. 3(a) that the blue wings of C iv λ 1549 and Lyα agree very poorly, probably causing overestimation of the N v λ 1240 strength, as in Q0000 – 398. The red wing of the Lyα profile is enhanced (Fig. 3c), but it is apparent from Fig. 3(d) that the asymmetry is not significant when compared with the magnitude of the errors.

*1256 – 175 (Fig. 4)*

The signal-to-noise ratio is lower than in the previous objects and identification of absorption features more difficult. In particular, in Fig. 4(a) the region from 3590–3640 Å could be explained by C iii λ 1175 emission at 3600 Å or blended absorption at 3620 Å. The second interpretation is the more likely but further data are required to provide confirmation. In Fig. 4(b) the amount of absorption in the violet wing of C iv λ 1549 is also uncertain and the smoothed profile may be low from 4650–4700 Å. This possibility should be considered when studying Fig. 4(c).

To within the limits of the errors (Fig. 4d) the profile (Fig. 4e) is symmetric and there is no shift between its peak and those of the other broad lines. It is interesting to note that the apparent slight asymmetry is in the opposite sense to that of the other QSOs, this is not surprising since the C iv λ 1549 wings match those of Lyα fairly well, reducing the tendency to overestimate the N v λ 1240 contribution to the blend.

*1331 + 170 (Fig. 5)*

There are no obvious problems in the smoothing of either the Lyα or C iv λ 1549 profiles in this object, but the C iv λ 1549 peak is at lower redshift than that for Lyα. A similar shift is present in the lower resolution data of Strittmatter *et al.* (1973) and so it is probably real. The synthetic blend (Fig. 5c) was formed by arbitrarily shifting the rest wavelength of C iv to 1546.1 Å thus correcting for the difference in redshift. Since there is invariably a mismatch between C iv λ 1549 and Lyα (see Section 4), this shift will introduce additional errors to the deblending process if N v λ 1240 is also shifted relative to Lyα. The excess emission at 3910 Å is probably Si ii λ 1263, inclusion of a component here in the synthetic blend made the fitting of N v λ 1240 impossible, perhaps because the Si ii λ 1263 feature is narrower than the C iv λ 1549 used to match it. Another possible cause of the bad fit is the presence of blended absorption lines in the region 3860–3900 Å in the 1216 blend (Fig. 5a). Apart from this possible Si ii λ 1263 emission the Lyα profile is symmetric to within the range of the error bars.

*Q2204 – 408 (Fig. 6)*

The C iv λ 1549 profile has a marked blue skew very similar to that of C iv λ 1549 in Q00207 – 398. O vi λ 1034 and Lyα are both heavily affected by absorption lines, but appear asymmetric in the same sense; N v λ 1240 is well blended with the broad Lyα feature and its shape not immediately discernible. Despite the forest of absorption lines, particularly around the peak, a reasonable fit was made to the 1216 feature (Fig. 6a). The slight enhancement in the C iv profile (Fig. 6b) at ~ 6330 Å may be due to blended absorption lines on either side of this region, the remainder of the profile is fairly unambiguous.

Although Lyα and C iv λ 1549 have similar profiles, a good fit to N v λ 1240 was not possible. This seems to be due to a combination of a strong red wing to Lyα, the poorly

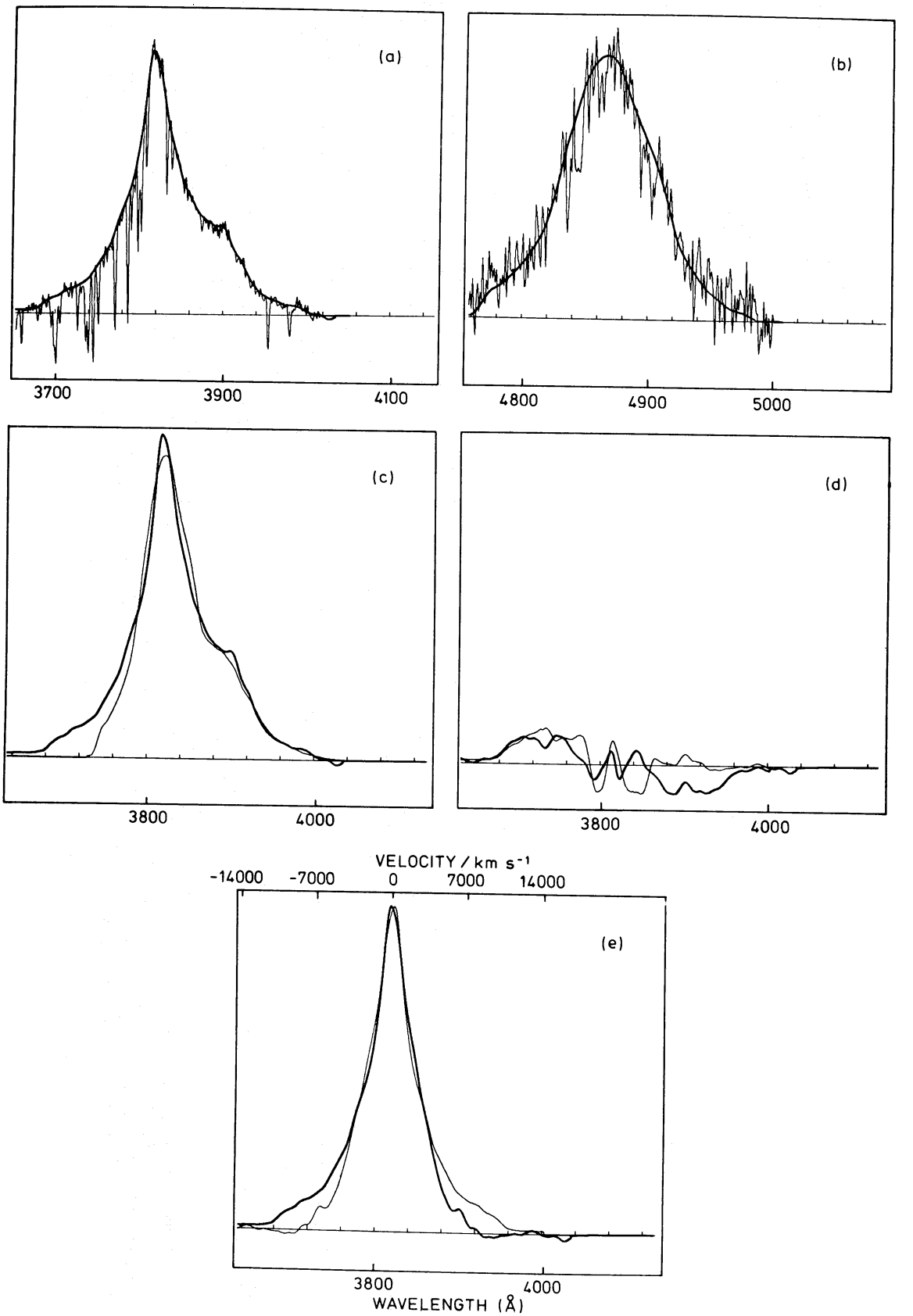


**Figure 3.** Line profile synthesis for Q1101 – 264. As Fig. 1. (a) Fit to 1216 blend, (b) fit to C IV λ 1549, (c) synthetic (feint) and fitted 1216 blends, (d) synthetic blend residuals (feint) and asymmetry in Lyα and (e) Lyα profile and its reflection (feint).

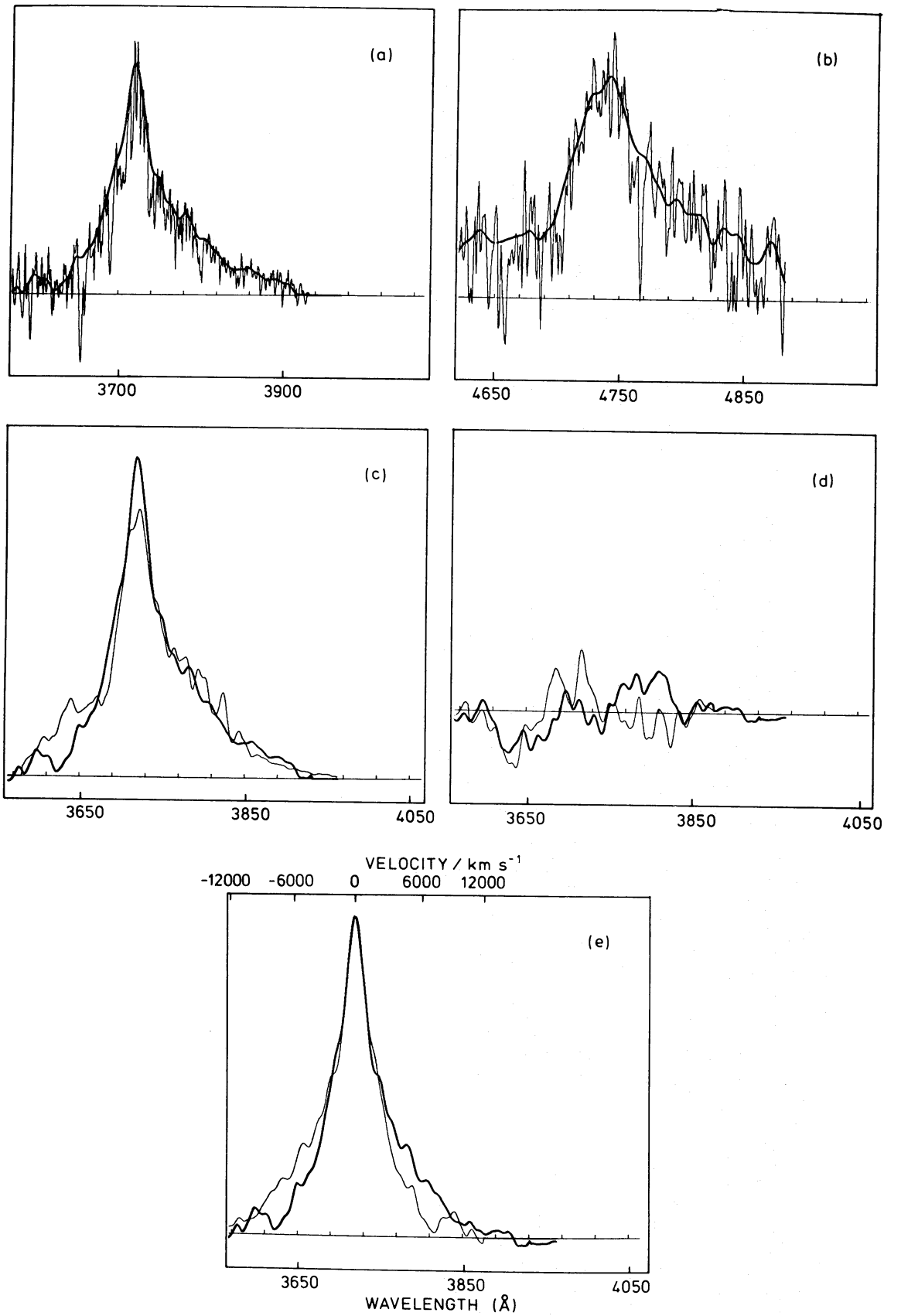


**Figure 4.** Line profile synthesis for 1256 – 175. As Fig. 1. (a) Fit to 1216 blend, (b) fit to C IV λ 1549, (c) synthetic (feint) and fitted 1216 blends, (d) synthetic blend residuals (feint) and asymmetry in Lyα and (e) Lyα profile and its reflection (feint).

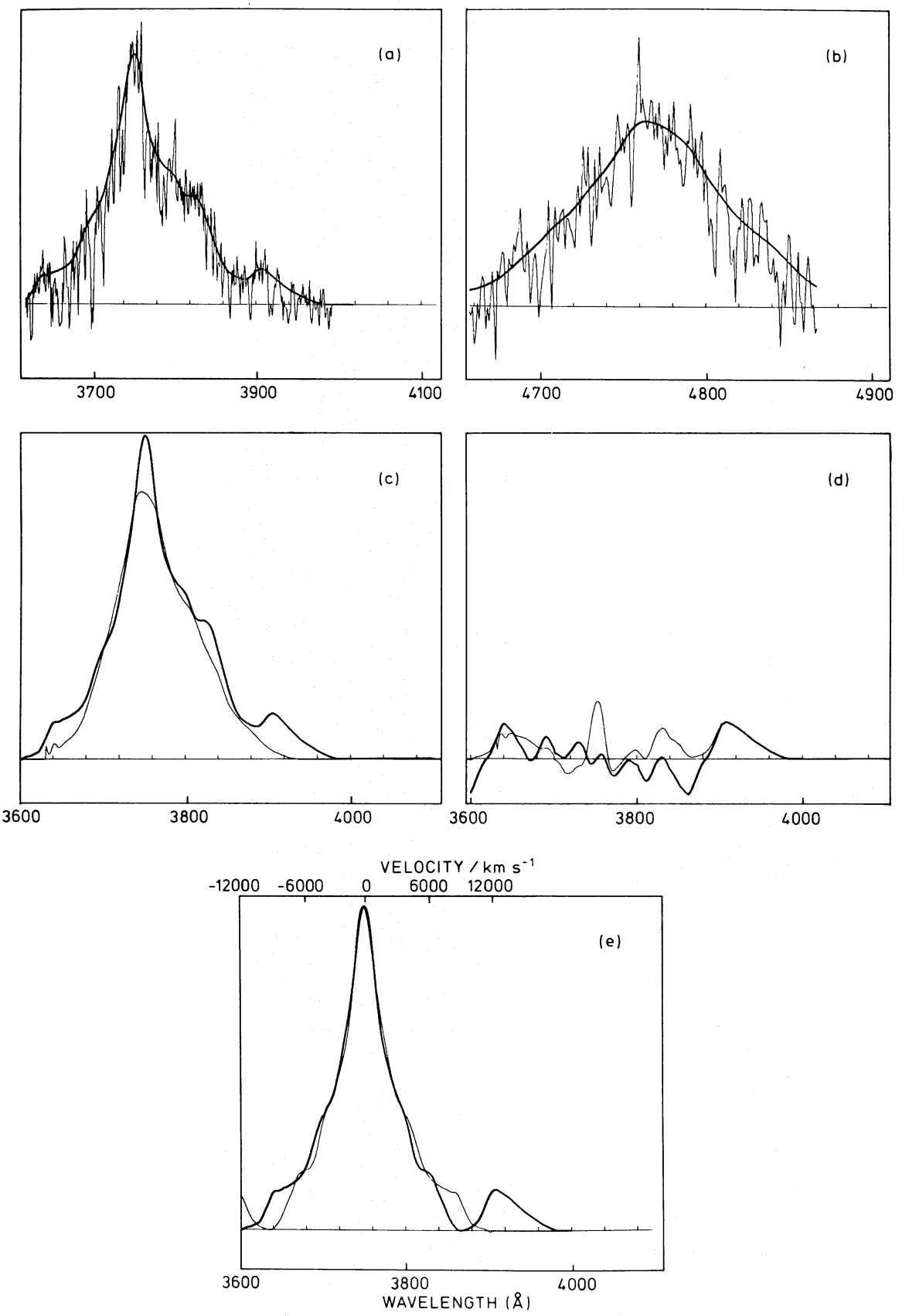


**Figure 5.** Line profile synthesis for 1331 + 170. As Fig. 1. (a) Fit to 1216 blend, (b) fit to C IV λ 1549, (c) synthetic (feint) and fitted 1216 blends, (d) synthetic blend residuals (feint) and asymmetry in Lyα and (e) Lyα profile and its reflection (feint).

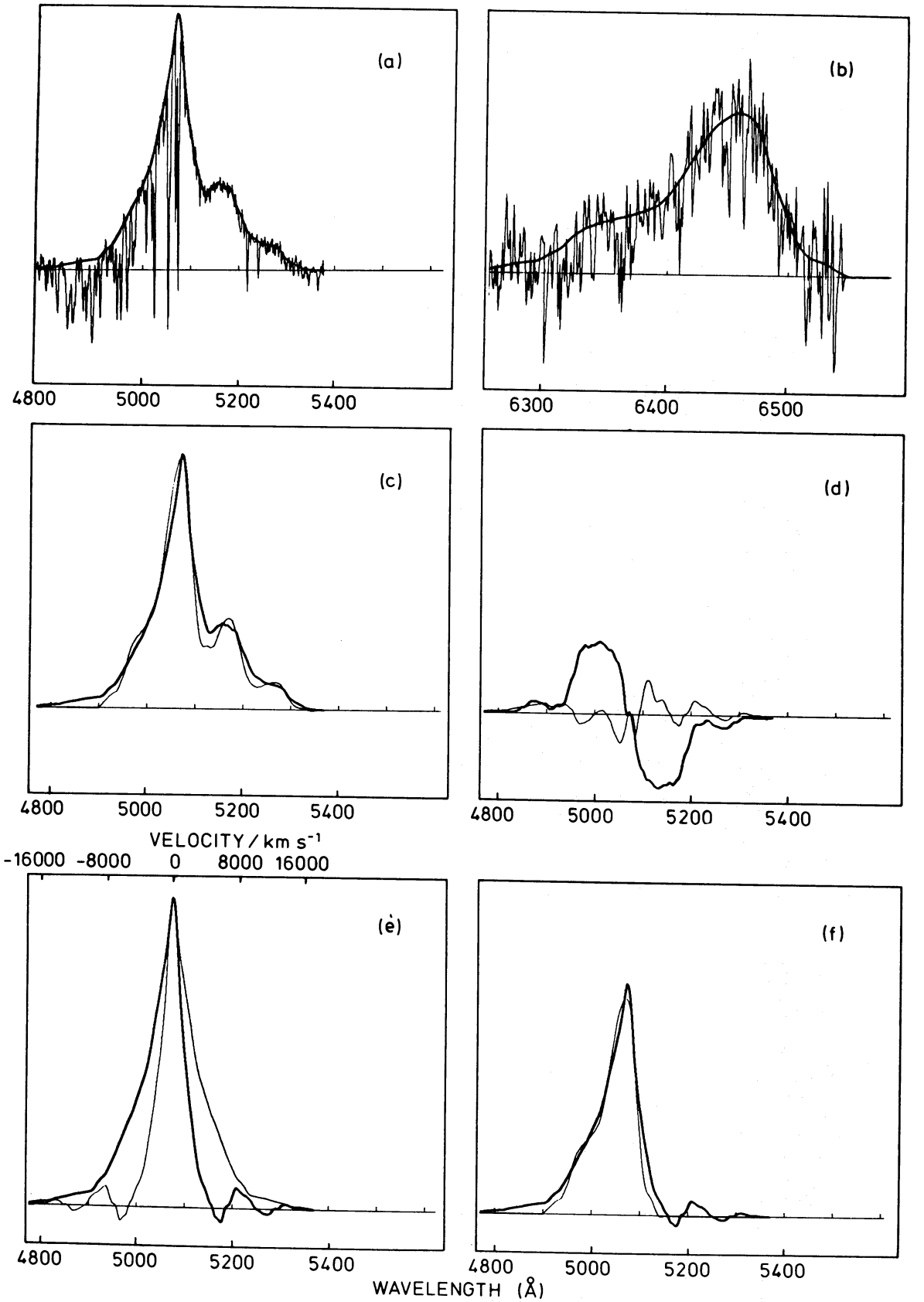


**Figure 6.** Line profile synthesis for Q2204 – 408. As Fig. 1. (a) Fit to 1216 blend, (b) fit to C IV λ 1549, (c) synthetic (feint) and fitted 1216 blends, (d) synthetic blend residuals (feint) and asymmetry in Lyα profile and its reflection (feint). Additionally, (f) a comparison of the Lyα profile (reinforced) with that for C IV λ 1549.

determined shape of the N v λ1240 feature and partly to the presence of Si II λ1263 emission. The final Lyα profile (Fig. 6e) is clearly enhanced in the blue wing; any errors due to blended absorption lines in fitting the blue wing will reinforce this asymmetry.

Fig. 6(f) shows a comparison, in the same velocity space, of C IV λ1549 (feint) with Lyα. The match is fairly good, with Lyα displaying a typical excess in its blue wing and the peaks matching more closely than is usual. The latter may be due to bad fitting of the absorption lines around the Lyα peak (Fig. 6a). This is the only example of strongly asymmetric Lyα emission in this sample and it appears that this QSO is relatively unusual in possessing such strongly asymmetric high-ionization lines. Since, if anything, the skew of Lyα is weaker than C IV λ1549, an explanation in terms of high-resonance line opacity in the neutral gas is impossible. The situation is discussed further below.

Uncertainties are introduced at each stage of the procedure outlined above and are best estimated by studying the line profiles utilized at each stage. There are two main sources of error.

(1) Although we are confident that most of the absorption lines are resolved, strong adjacent lines may be blended in the wings and thus depress the apparent continuum; this is more of a problem in Lyα than C IV λ1549.

(2) The production of a good synthetic blend of the Lyα 1216 feature, as well as being dependent on the accuracy of the smoothing process, also relies upon the similarity of the profiles involved. As we have seen, Lyα generally has broader wings and a sharper peak than C IV. Since an accurate match to the N v λ1240 emission was the first priority, the synthetic blend was chosen to fit thde main part of the profile rather than the peak and wings. Consequently, in the red wing it is difficult to distinguish between the real wing of Lyα and Si II λ1263 emission. Possible differences between the N v λ1240 and C IV λ1549 profiles further increase these problems. In addition, since the N v λ1240 strength was boosted to match the red wing of the 1216 blends, without making any allowance for differences between the C IV λ1549 and Lyα profiles, it is likely that its contribution is overestimated and the final Lyα profile enhanced in its blue wing.

The significance of the asymmetries appearing in plates (e) is indicated by studying the corresponding plate (d). This displays, on the same scale as (c) and (e) the subtraction of the Lyα profile from its reflection (reinforced line), (anti-symmetric about the line centre) and that of the observed 1216 feature and the synthetic blend (feint). The latter is a measure of the uncertainties in the deblending and subtraction of N v λ1240: the blue half of this is indicative of the difference between Lyα and C IV λ1549 only; the red half, because of the presence of N v λ1240 and Si II λ1263, combines the differences in all three profiles. The Lyα asymmetry was considered real only if its scale, judged from the subtracted profile, was clearly in excess of the error term in both wings of the line.

## 4 Discussion

The C IV λ1549 line tends to be weaker in both the wings and central peak than Lyα λ1216; this is particularly noticeable in Figs 1(c) and 3(c) for Q0000 – 398 and Q1101 – 264 respectively. These results are not inconsistent with the earlier conclusion of Baldwin & Netzer (1978) that the profiles are similar, since the subtle differences apparent in the present data sample would be masked in their lower-resolution spectra.

The Lyα emission line appears to be symmetric in all but one of the QSOs in the small sample we have observed. In the exceptional object, Q2204 – 408, the Lyα and C IV λ1549 profiles appear to have a similar flux excess to short wavelengths. The discrepancy between C IV and Lyα λ1216 profiles is probably the cause of the tendency towards a slightly en-

hanced blue wing in the final Lyα profiles as a consequence of overestimating the N v λ 1240 strength. In only one case, 1331 + 170, is there any redshift difference between Lyα and the other ultraviolet lines; however, the C iv λ 1549 and Lyα profiles compare favourably with those of Q0000 − 398 and Q1101 − 264. Following the arguments outlined earlier, these results imply that, if Lyα originates mainly in optically-thick clouds through recombination and collisional excitation on the surface facing the QSO, the motion of these clouds is not predominantly radial. If it were, the levels would radiate anisotropically in Lyα and marked asymmetry in the observed profiles would be expected.

Possible mechanisms for obtaining isotropically radiating optically-thick clouds have recently been discussed by Mathews (1982); these include modification of the shape of the clouds, internal gas motions and possible non-radiative effects. Another alternative is that most of the Lyα photons originate predominantly in optically-thin gas clouds (Blumenthal & Mathews 1979). There is then little or no opacity to Lyα photons, the emissivity of each cloud is directionally independent and the corresponding emission line symmetric for any axisymmetric gas velocity distribution. Photo-ionization calculations (e.g. Davidson & Netzer 1979; Carswell & Ferland 1980) indicate that a cloud system of this type yields relatively weak low-ionization lines. In order to reproduce the observations, an additional optically-thick component to the cloud distribution must be invoked. This component will also be the source of most of the Balmer emission (Kwan & Krolick 1981) and the low-ionization lines from e.g. O i and Mg ii. Thus, to avoid introducing asymmetry, either the Lyα emission from this region must be relatively weak or else there is little or no radial motion. Of course, if the generally accepted concept of large number of clouds is abandoned, it is possible to contrive symmetric Lyα profiles from radial motion coupled with asymmetric velocity or cloud distributions.

Another observational trend which is present in this data is that the redshift of low-ionization lines (see Section 3) e.g. O i λ1304, C ii λ 1335, is high relative to the high-ionization lines by velocities of order 1000 km $s^{-1}$ (Table 3). Shifts of this nature cannot be produced by any axisymmetric distribution of randomly orbiting clouds. A radial component to their motion, coupled with some form of positionally dependent obscuration, is required. The suggestive evidence that their profiles are relatively narrow provides further evidence for variations of cloud velocity with distance from the central source. It is clear that in order to generate both a symmetric Lyα profile and shifts some form of compromise must be invoked.

Additionally, any model attempting to reproduce the above phenomena must have sufficient flexibility to be able to plausibly explain anomalies such as those apparent in this small sample.

(a) *Q0207 − 398:* High-ionization lines are strongly asymmetric while Lyα and low-ionization lines are symmetric. The peak of Lyα is at rest relative to that of C iv λ 1549 and other low-ionization lines are shifted (see Table 3).

(b) *1331 + 170:* C iv λ 1549 is blueshifted relative to Lyα although both profiles appear summetric and no more dissimilar than typically found in this sample (Table 3).

(c) *Q2204 − 408:* All the lines have greatly enhanced blue wings.

There are two main mechanisms for substantially obscuring emission within a broad-line region cloud: (i) high line opacity and (ii) dust or other sources of continuum opacity (such as Balmer continuum).

(i) Line opacity: the generating function for a high-ionization line, such as C iv λ 1549, is uniform over its production region and the line opacity minimal elsewhere. This is not true for the Lyα line for the reasons discussed earlier.

(ii) The quantity of dust in the broad-line region in QSOs has been discussed by many authors, in particular Baldwin & Netzer (1978), London (1979), Ferland & Netzer (1979), Martin & Ferland (1980), Davidson & Netzer (1979) and is generally believed to be small (~ 10 per cent of that in our Galaxy). Since the opacity of dust over the wavelength region in question is fairly uniform, qualitatively at least, a system of optically-thick, dusty, infalling gas clouds could give rise to spectra lines such as those observed in Q2204 – 408, though a larger amount of dust is probably required. In this picture, the symmetry of the Lyα line in Q0207 – 398, would require that most of this line be formed in optically-thin clouds and the relative redshift of O I λ1304 and C II λ1335 in both objects implies that these lines come from yet another region of the cloud distribution. In any case, it appears that these QSOs are unusual in possibly having both dust and radial motion when most exhibit little evidence for either.

Other sources of continuum opacity, such as Balmer continuum, similarly affect lines at similar wavelengths, so the differences between Lyα and O I, for example, are rather hard to explain. However, in both cases, if the lines come from different cloud populations they may be subject to differing continuum absorption.

## 5 Conclusions

(1) Lyα is generally symmetric so either there is little radial motion in the gas or most of the Lyα is formed in optically-thin clouds.

(2) The shapes of the emission lines vary substantially from object to object.

(3) Detailed profiles of the broad lines in the same objects do not match, especially C IV λ1549 and Lyα.

(4) From this brief, qualitative, discussion it is apparent that no simple model can explain the observations. A wide range of cloud sizes, a complex velocity distribution and some combination of the above obscuration mechanisms will no doubt cover most aspects of the present data. The value of a detailed model based on such a small sample of spectra is questionable and its discussion beyond the scope of the present paper.

(5) Low-ionization lines such as O I λ1304 are redshifted and may be narrower than 'high-ionization' lines such as C IV and Lyα.

It is essential that more high-resolution data be obtained in order to estimate how typical are the profiles here described. It is also very important to obtain good line profiles for as many lines as possible in a single object, e.g. C IV λ1549 to Hα when sensitive low-noise red detectors become available for spectroscopic work or using the space telescope.

## Acknowledgments

We are grateful to Alec Boksenberg and Malcolm Smith for the use of some data obtained with them for another project, to Dave Hanes and the AAO staff for assistance at the telescope and to a referee for many useful comments. Financial support from SERC is also gratefully acknowledged.

## References

Allen, D. A., Barton, J., Gillingham, P. & Carswell, R. F., 1982. *Mon. Not. R. astr. Soc.*, **200**, 271.
Atwood, B., Baldwin, J. A. & Carswell, R. F., 1982. *Astrophys. J.*, in press.
Baldwin, J. A. & Netzer, H., 1978. *Astrophys. J.*, **226**, 1.

Blumenthal, G. R. & Mathews, W. G., 1979. *Astrophys. J.*, **233**, 479.
Boksenberg, A., 1972. *Proceedings ESO/CERN Conference*, p. 295, eds Lausten, S. & Reiz, A., Geneva.
Boksenberg, A., 1978. *Proceedings Symp. of 26th Plenary Meeting of COSPAR*, p. 29, eds van der Hucht, K. A. & Viana, G., Pergamon Press, Oxford.
Carswell, R. F., Hillard, R. L., Strittmatter, P. A., Taylor, D. J. & Weymann, R. J., 1975. *Astrophys. J.*, **196**, 351.
Carswell, R. F. & Ferland, G. J., 1980. *Mon. Not. R. astr. Soc.*, **191**, 55.
Carswell, R. F., Whelan, J. A. J., Smith, M. G., Boksenberg, A. & Tytler, D., 1982. *Mon. Not. R. astr. Soc.*, **198**, 91.
Davidson, K., 1972. *Astrophys. J.*, **171**, 213.
Davidson, K., 1977. *Astrophys. J.*, **218**, 20.
Davidson, K. & Netzer, H., 1979. *Rev. Mod. Phys.*, **51**, 715.
Ferland, G. J. & Netzer, H., 1979. *Astrophys. J.*, **229**, 274.
Ferland, G. J., Netzer, H. & Shields, G. A., 1979. *Astrophys. J.*, **232**, 382.
Gaskell, C. M., 1981. *PhD thesis*, University of California, Santa Cruz.
Gaskell, C. M., 1982. *Astrophys. J.*, in press.
Kwan, J. & Krolick, J. H., 1981. *Astrophys. J.*, **250**, 478.
London, R., 1979. *Astrophys. J.*, **228**, 8.
MacAlpine, G. M., 1976. *Astrophys. J.*, **204**, 694.
Martin, P. G. & Ferland, G. J., 1980. *Astrophys. J.*, **235**, L125.
Mathews, W. G., 1982. *Astrophys. J.*, **252**, 39.
Netzer, H., 1976. *Mon. Not. R. astr. Soc.*, **177**, 473.
Netzer, H., 1977. *Mon. Not. R. astr. Soc.*, **178**, 489.
Oke, J. B., 1974. *Astrophys. J. Suppl.*, **27**, 21.
Osmer, P. S., 1979. *Astrophys. J.*, **227**, 18.
Osmer, P. S. & Smith, M. G., 1976. *Astrophys. J.*, **210**, 267.
Osmer, P. S. & Smith, M. G., 1977. *Astrophys. J.*, **213**, 607.
Shields, G. A., Oke, J. B. & Sargent, W. L. W., 1972. *Astrophys. J.*, **176**, 75.
Smith, M. G., Carswell, R. F., Whelan, J. A. J., Wilkes, B. J., Boksenberg, A., Clowes, R. G., Savage, A., Cannon, R. D. & Wall, J. V., 1981. *Mon. Not. R. astr. Soc.*, **195**, 437.
Strittmatter, P. A., Carswell, R. F., Burbidge, E. M., Hazard, C., Baldwin, J. A., Robinson, L. & Wampler, E. J., 1973. *Astrophys. J.*, **183**, 767.
Strittmatter, P. A. & Williams, R. E., 1976. *A. Rev. Astr. Astrophys.*, **14**, 307.
Whelan, J. A. J., Smith, M. G. & Carswell, R. F., 1979. *Mon. Not. R. astr. Soc.*, **189**, 363.